## Supporting Information Appendix

**Table S1** qRT-PCR primer sequences (Integrated DNA Technologies, Coralville, IA, USA)

| | **Forward** | **Reverse** |
|---|---|---|
| ***GAPDH*** | GGAGCGAGATCCCTCCAAAAT | GGCTGTTGTCATACTTCTCATGG |
| ***GAPDH*** | ACAACTTTGGTATCGTGGAAGG | GCCATCACGCCACAGTTTC |
| ***SOX2*** | GCCGAGTGGAAACTTTTGTCG | GGCAGCGTGTACTTATCCTTCT |
| ***SOX2*** | TGGACAGTTACGCGCACAT | CGAGTAGGACATGCTGTAGGT |
| ***OLIG2*** | CCAGAGCCCGATGACCTTTTT | CACTGCCTCCTAGCTTGTCC |
| ***OLIG2*** | TGGCTTCAAGTCATCCTCGTC | ATGGCGATGTTGAGGTCGTG |
| ***SALL2*** | CAGCGGAAACCCCAACAGTTA | GAGGGTCAGTAGAACATGCGT |
| ***SALL2*** | GCCTGAGGGTCACAATAATCC | TGGCAGCGACCAGGAAATG |
| ***POU3F2*** | CGGCGGATCAAACTGGGATTT | TTGCGCTGCGATCTTGTCTAT |
| ***POU3F2*** | AAGCGGAAAAAGCGGACCT | GTGTGGTGGAGTGTCCCTAC |

**Table S2** siRNA duplex sequences (Millipore Sigma, Billerica, MA, USA)

| | **Sense** | **Antisense** |
|---|---|---|
| ***SOX2*** | CAGUAUUUAUCGAGAUAAA[dT][dT] | UUUAUCUCGAUAAAUACUG[dT][dT] |
| ***SOX2*** | CCACCUACAGCAUGUCCUA[dT][dT] | UAGGACAUGCUGUAGGUGG[dT][dT] |
| ***SOX2*** | GGUAGGAGCUUUGCAGGAA[dT][dT] | UUCCUGCAAAGCUCCUACC[dT][dT] |
| ***OLIG2*** | GGACUAUCCUUUAAAGGUA[dT][dT] | UACCUUUAAAGGAUAGUCC[dT][dT] |
| ***OLIG2*** | UACCUUUAAAGGAUAGUCC[dT][dT] | UUUGCCUAUAUGAAAGAAC[dT][dT] |
| ***OLIG2*** | CGGAUCAAACUGGGAUUUA[dT][dT] | UAAAUCCCAGUUUGAUCCG[dT][dT] |
| ***SALL2*** | GAUGUUCUCUCCGGGACCU[dT][dT] | AGGUCCCGGAGAGAACAUC[dT][dT] |
| ***SALL2*** | GGACAAGAAGCAAAUGACA[dT][dT] | UGUCAUUUGCUUCUUGUCC[dT][dT] |
| ***SALL2*** | GGAUGUUCCUUCUUCAACA[dT][dT] | UGUUGAAGAAGGAACAUCC[dT][dT] |
| ***POU3F2*** | CUCAGAAUAUUGCUGCUCU[dT][dT] | AGAGCAGCAAUAUUCUGAG[dT][dT] |
| ***POU3F2*** | GCAGAAACAGCUUCACAAA[dT][dT] | UUUGUGAAGCUGUUUCUGC[dT][dT] |
| ***POU3F2*** | GCACAAUUCACUGACCCAA[dT][dT] | UUGGGUCAGUGAAUUGUGC[dT][dT] |
| **Universal Negative Control** | GGUUUACAUGUUCCAAUAU[dT][dT] | AUAUUGGAACAUGUAAACC[dT][dT] |

**Table S3** List of Antibodies

| Antigen | Species | Dilution | Vendor |
|---|---|---|---|
| human NESTIN | Rabbit | 1:1000 for ICC, 1:5000 for Western Blotting | Millipore Sigma |
| EEA1 | Rabbit | 1:500 for ICC | Cell Signaling |
| RAB5 | Rabbit | 1:500 for ICC | Cell Signaling |
| RAB7 | Rabbit | 1:500 for ICC | Cell Signaling |
| GFAP | Mouse | 1:500 for ICC | Cell Signaling |
| GALC | Mouse | 1:500 for ICC | Cell Signaling |
| TUJ1, NFM | Rabbit | 1:500 for ICC | Millipore Sigma |
| SOX2 | Rabbit | 1:500 for ICC, 1:1000 for Western Blotting | Millipore Sigma |
| OLIG2 | Rabbit | 1:500 for ICC, 1:1000 for Western Blotting | Millipore Sigma |
| SOX2 | Mouse | 1:500 for ICC, 1:1000 for Flow Cytometry | R&D Systems |
| OLIG2 | Mouse | 1:500 for ICC, 1:1000 for Flow Cytometry | R&D Systems |
| Rabbit Whole IgG | Rabbit | 1:500 for ICC, 1:1000 for Western Blotting | Biolegend |
| β-ACTIN | Mouse | 1:1000 for ICC, 1:1000 for Western Blotting | Santa Cruz Biotechnology |
| CD31 | Rat | 1:1000 for ICC | Santa Cruz Biotechnology |
| VE Cadherin | Goat | 1:1000 for ICC | Santa Cruz Biotechnology |
| SALL2 | Rabbit | 1:1000 for ICC, 1:1000 for Western Blotting | Bethyl Laboratories |
| POU3F2 | Rabbit | 1:1000 for ICC, 1:1000 for Western Blotting | Bethyl Laboratories |
| Isotype IgG1κ | Mouse | 5µl / million cells for Flow Cytometry | BioLegend |
| CD133-PE | Mouse | 5µl / million cells for Flow Cytometry | Milteny Biotec |
| Isotype IgG1κ-PE | Mouse | 5µl / million cells for Flow Cytometry | Milteny Biotec |
| Isotype IgG1κ-FITC | Mouse | 5µl / million cells for Flow Cytometry | Milteny Biotec |

## SI Figures

**Figure S1** Patient tissue analysis of TF expression profiles via Ivy Glioblastoma Atlas Project database. To identify the appropriate nano RNAi delivery route to treat malignant BTICs in the brain, the Ivy Glioblastoma Atlas Project (Ivy GAP) collection of patient tissue profiles offer detailed RNAseq, gene expression, and *in situ* hybridization (ISH) profiles from GBM patients. **A.** Microdissection based RNAseq data with pathology features or gene expression characteristics show clustering of high expression of TFs in cellular tumor regions, but not in the blood vessel associated regions, perinecrotic zones, or pseudopalisading cells. The expressions in the leading edge or infiltrating segments were in consistent across the TFs. **B** & **C.** ISH examples of OLIG2 and SOX2 mRNA enrichment can been seen in cellular tumor regions (red arrows), but not in vasculature-rich regions. These indicate that the ideal siRNA-NP complex delivery route should be intratumoral, rather than systemic that requires passage through the brain vasculature.

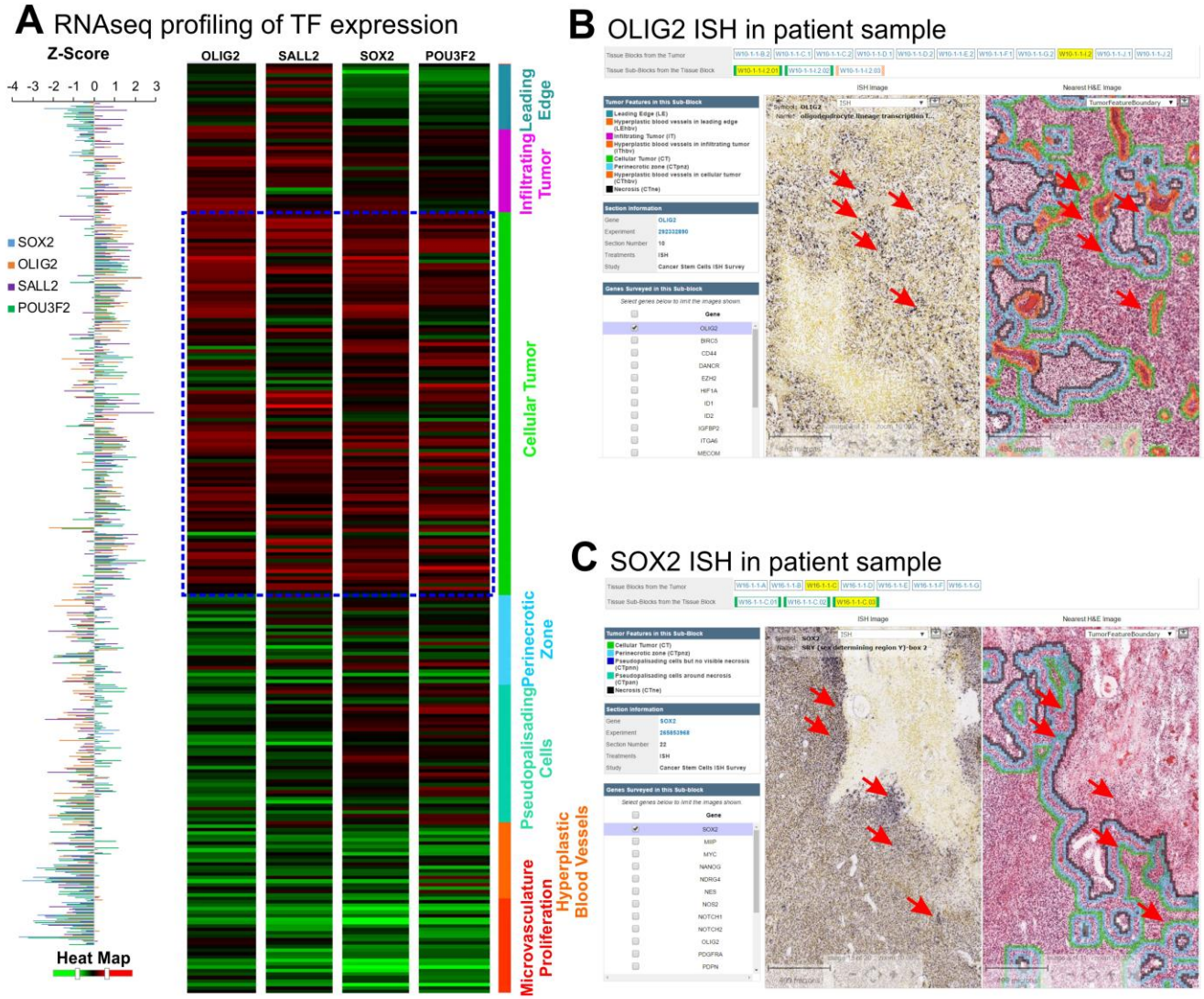

**Figure S2** BTIC TF expression profiling. One of the original GBM cell lines, MGG8, used to identify the 4 TFs responsible for the hierarchical programmability of BTICs, was one of the BTIC models tested for differentiation and TF expression induction via serial lentiviral transduction of the 4 core TFs. **A**. The induced counterpart, known as the iTPCs (for induced tumor propagating cells) have high levels of TF expression, and was used as the reference cell line to gauge the levels of relative expression of TFs in patient derived BTIC cells. Based on the induced TF expression levels in iTPC cells, the relative expression levels of SOX2 is shown through qRT-PCR. **B.** Based on the average mRNA expression levels of the 4 master TFs relative to iTPC TF mRNA levels, two cell lines (MGG8 and GBM43) were identified to represent the optimal TF siRNA KD target models, as they significantly express higher average master TF levels based on qRT-PCR analysis (n=4; ***p<0.001, t test).

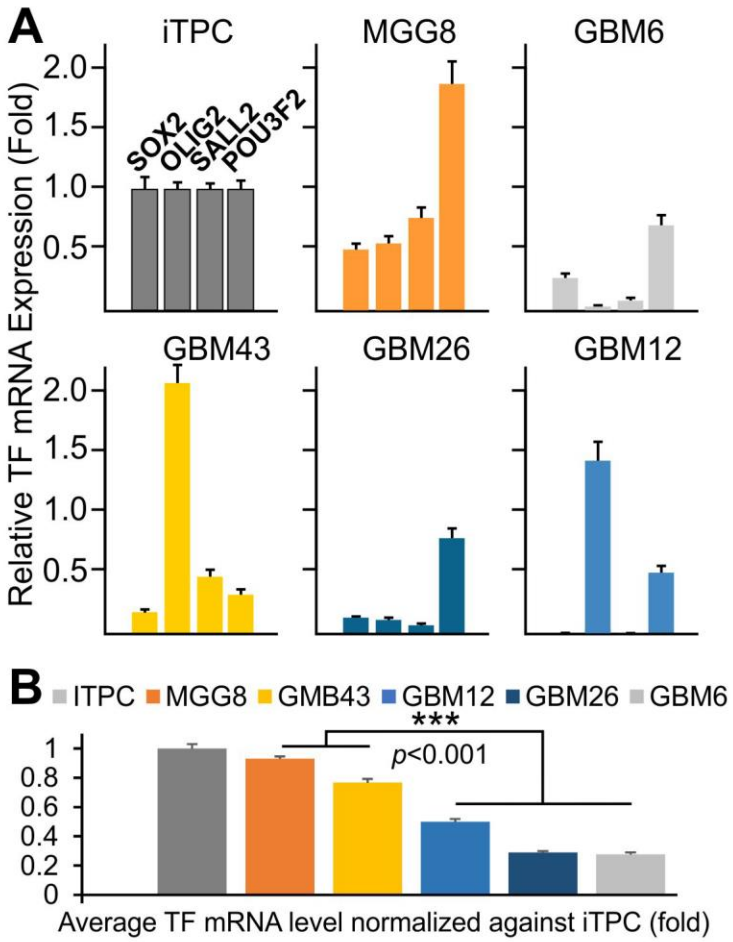

**Figure S3** Original Li-Cor Western blotting images of: **A**. Cell line comparison of the TF expression; **B**. Combo siRNA knockdown of master TFs in MGG8 and GBM43; **C**. The original Western blotting images of LPNP-siRNA combo knockdown of TFs in MGG8, compared with LPNP encapsulated single TF siRNA knockdown.

**A** Original Li-Cor Western Blots for Figure 1

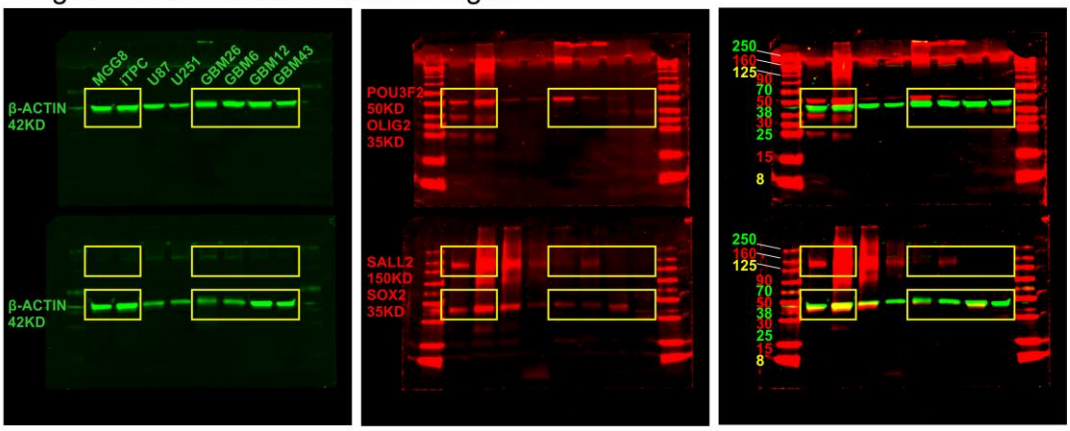


**B** Original Li-Cor Western Blots for Figure 2

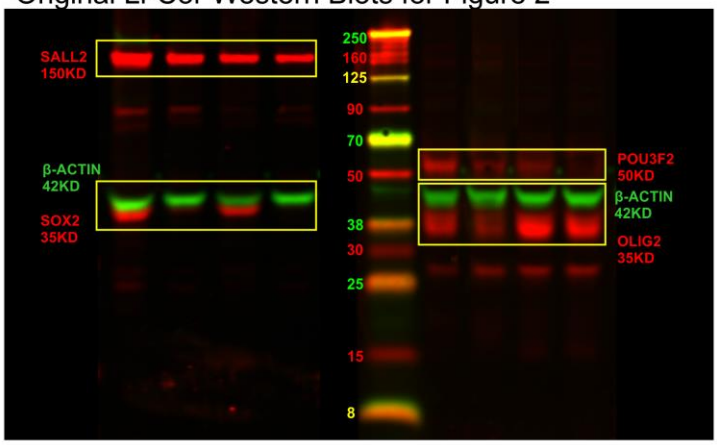


**C** Original Li-Cor Western Blots for Figure 5

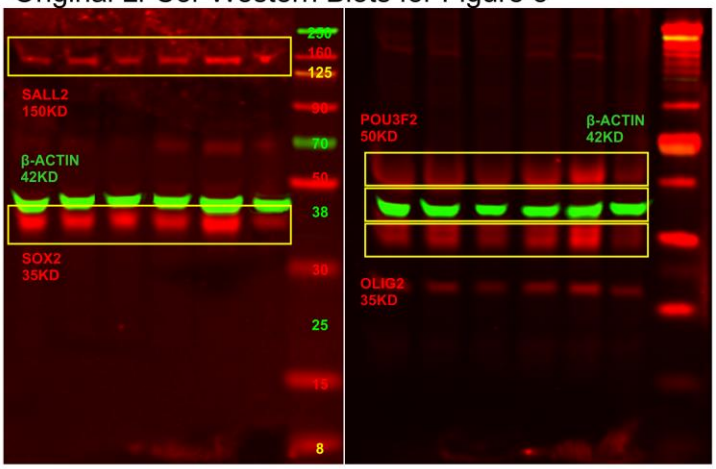

**Figure S4** The effect of combo TF siRNA knockdown on core TF expression in BTICs. To validate the impact of combo siRNA knockdown of the core TFs in BTICs, dual staining of pairs of core TFs were done using BTICs treated with either the control siRNA or the combo siRNAs. After 72h, fluorescent microscopy indicates successful knockdown of the TF protein expression levels in BTICs treated with combo siRNAs, but not in BTICs treated with the control siRNA.

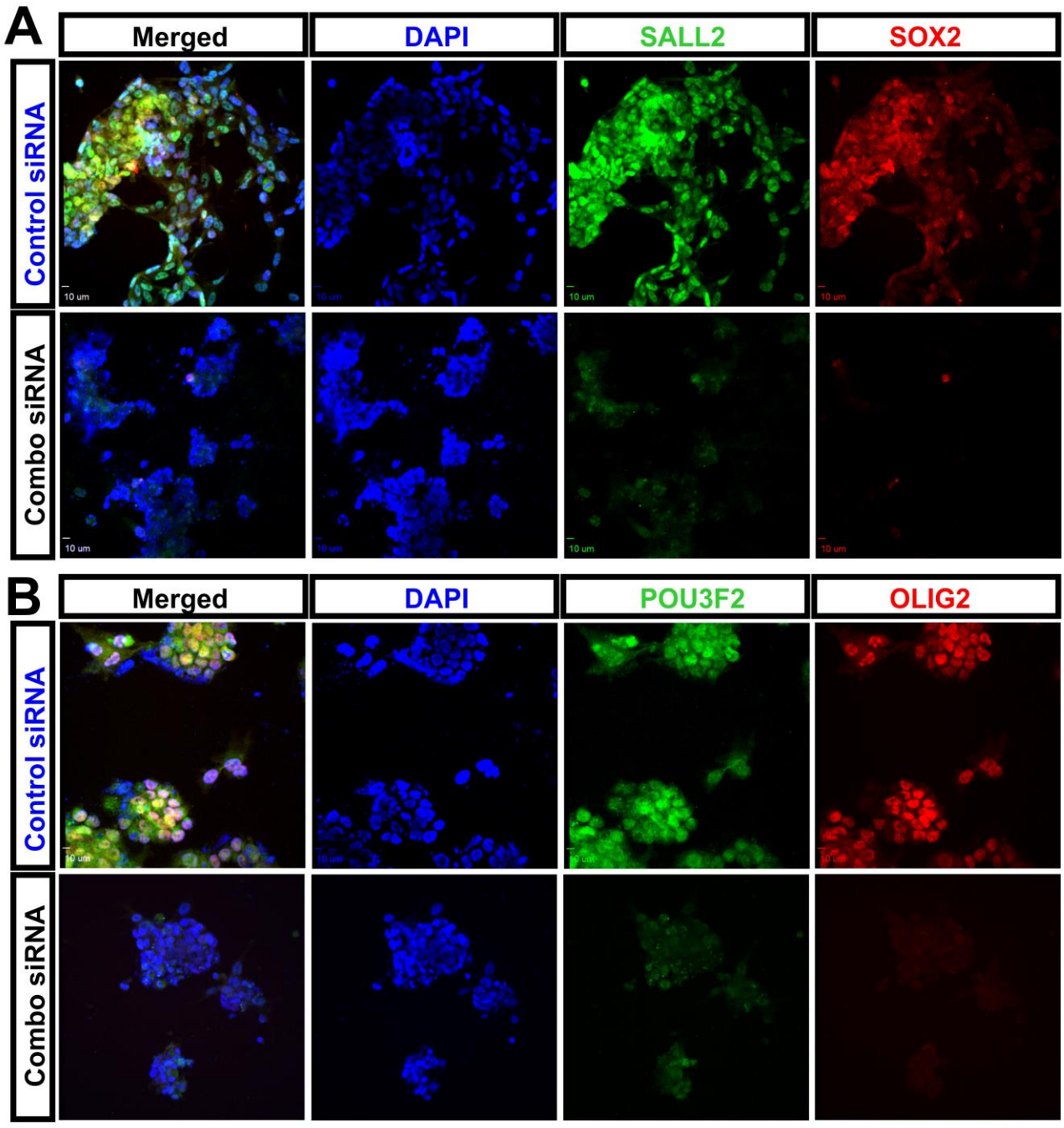

**Figure S5** The enlarged view of the super resolution Single Molecule Localization Microscopy (SMLM) images of endosomes (green) and endocytosed siRNA-LPNPs (red).

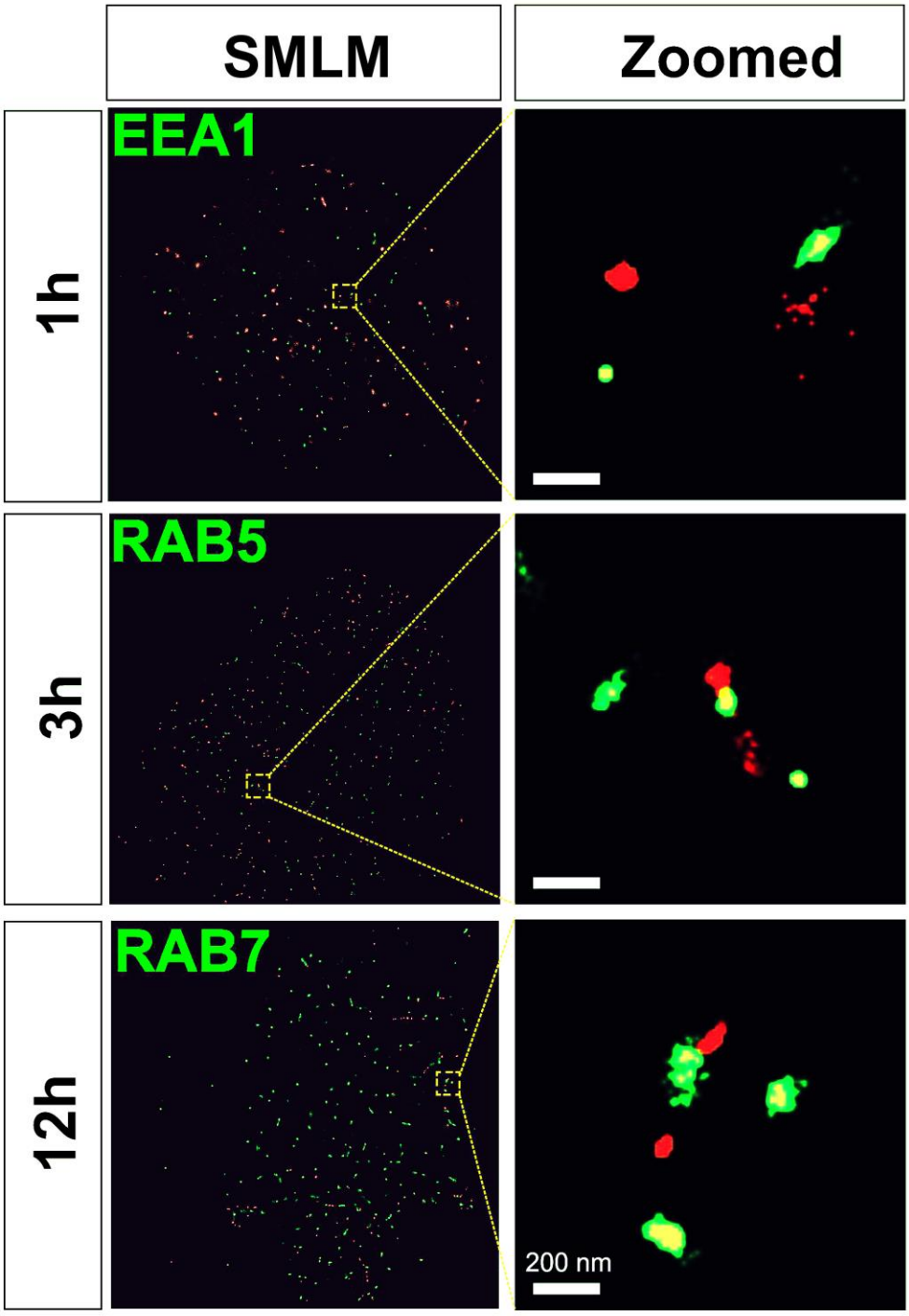

**Figure S6** The CellSimple™ flow cytometry assay assessment of cell proliferation capabilities using the Click-iT EdU assay kit. **A.** Human astrocytes are terminally differentiated cell types and extremely low proliferation can be revealed by 1 hour EdU incubation, and the differences between siRNA-LPNP treatments are too small for meaningful comparison. **B & C.** With only 1 hour EdU incubation, the reduction of proliferative capacity after 24 h siRNA-LPNP treatment is significantly observable in a dose-dependent fashion to increasing doses of combo siRNA for both MGG8 and GBM43 BTICs (n=3; ***$p$<0.001, t test).

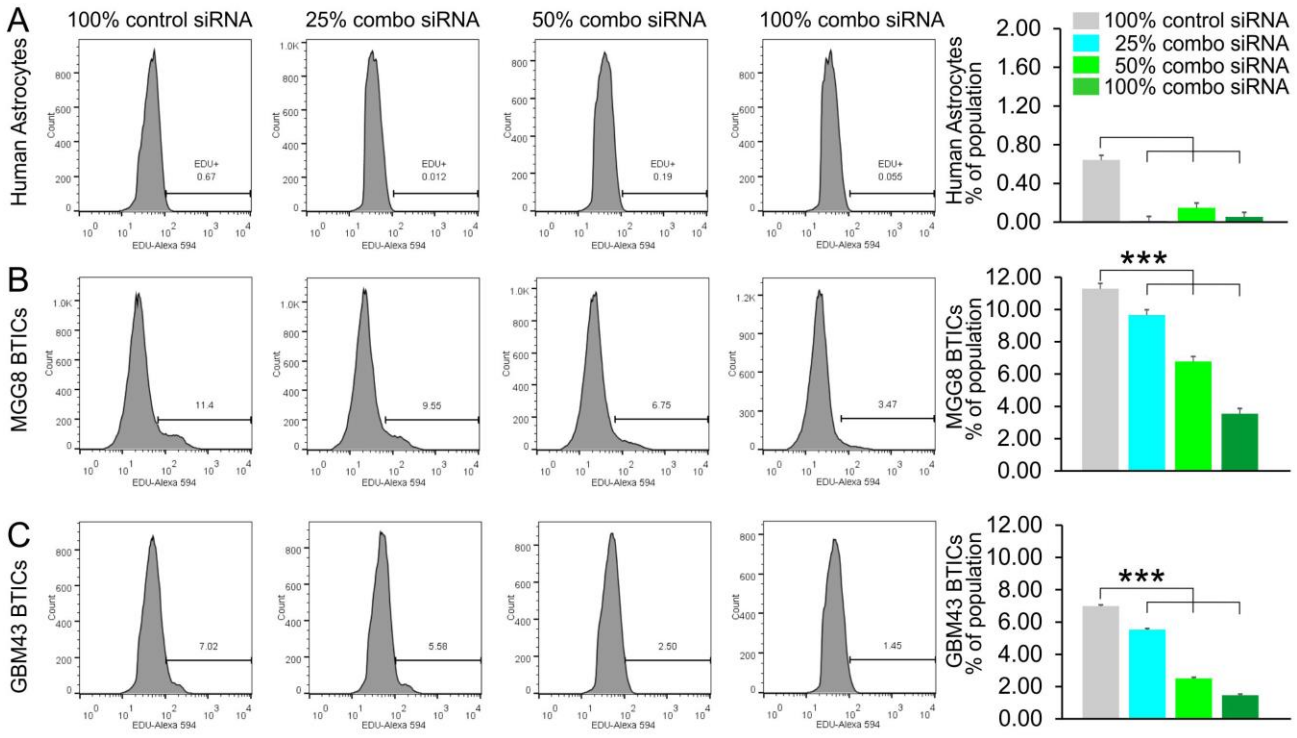


**Figure S7** The Ki67 flow cytometry assay assessment of cell proliferation capabilities. The impact of combo siRNA encapsulated in LPNPs on BTIC proliferation can been confirmed via the Ki67 flow cytometry. **A.** Using anti-rabbit IgG isotype antibody to define the gate, combo siRNA dose-dependently reduced the population in MGG8 BTICs showing positive Ki67 stain after 24 h of treatment. **B.** Significant differences were observed between control siRNA treatment and various doses of combo siRNA (n=3; ***$p$<0.001, t test).

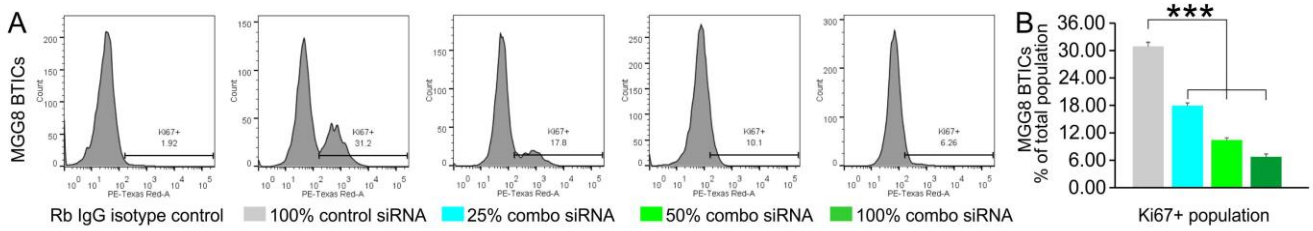

**Figure S8** The CellSimple™ Annexin V apoptosis detection assay. **A.** Using human astrocytes as controls, we observed low toxicity at increasing doses of combo siRNA encapsulated in LPNP for 24 h, but there was slightly increased necrotic and late apoptotic dead populations at 5μg total combo siRNA treatment. **B.** MGG8 BTICs show good tolerance to the total 5μg siRNA treatment, but the full dosing of combo siRNA led to increased necrotic cell death. **C.** GBM43 BTICs demonstrate different response profile to the siRNA-LPNP therapy, in that a discernable early apoptotic population was observed with the full 5μg of control siRNA dosing, and the apoptotic population continues to rise with increasing dosing composition of the combo siRNAs in the total 5μg of siRNA-LPNP treatment, with less pronounced necrosis as part of the outcome (n=3; ***$p$<0.001, t test).

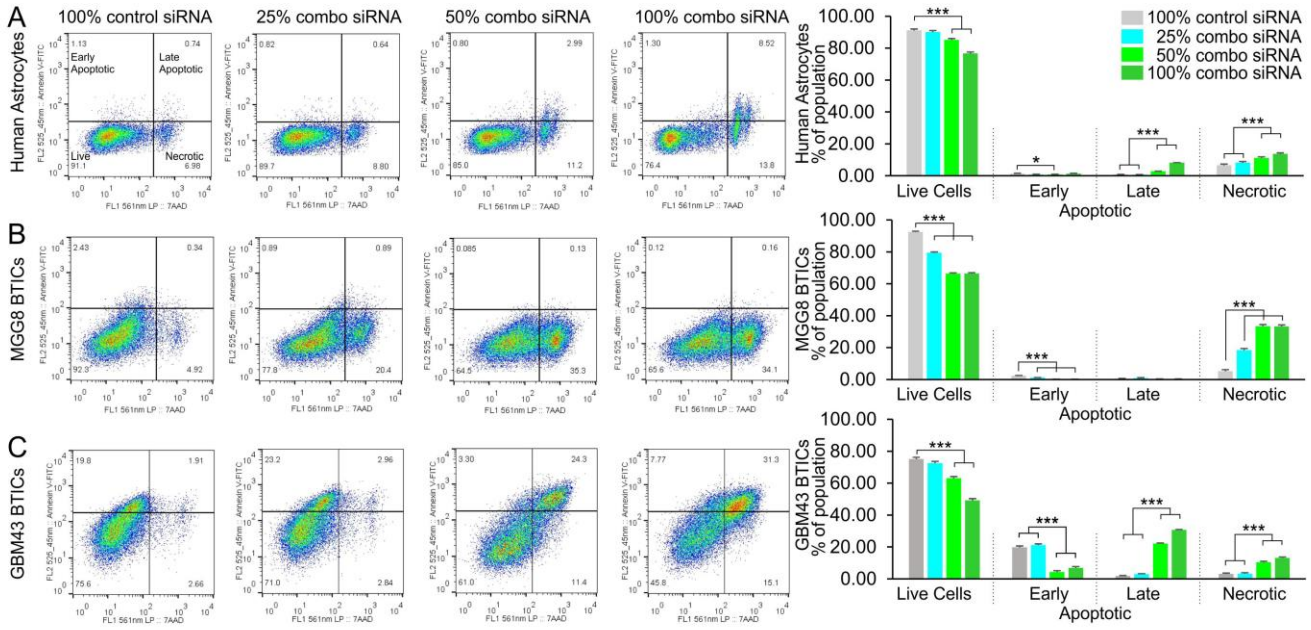

**Figure S9** The effect of siRNA-LPNP complexes on TF expression *in vivo.* To ensure that the effects of TF siRNA-LPNPs mirrors the *in vitro* validations, MGG8-mCherry xenografts were implanted in mouse brains, and received either universal non-targeting control siRNA-LPNP complexes or combination siRNA-LPNP complexes against the 4 TFs via the subcutaneous osmotic pump. Mouse brains were then collected and processed for immunocytochemistry after 4 days of therapy. The TF expression levels were uniformly high (white signals) in the brains that received control siRNAs, whereas the TF expression levels were abolished in MGG8-mCherry xenografts in the brains receiving combo TF siRNA-NPs.

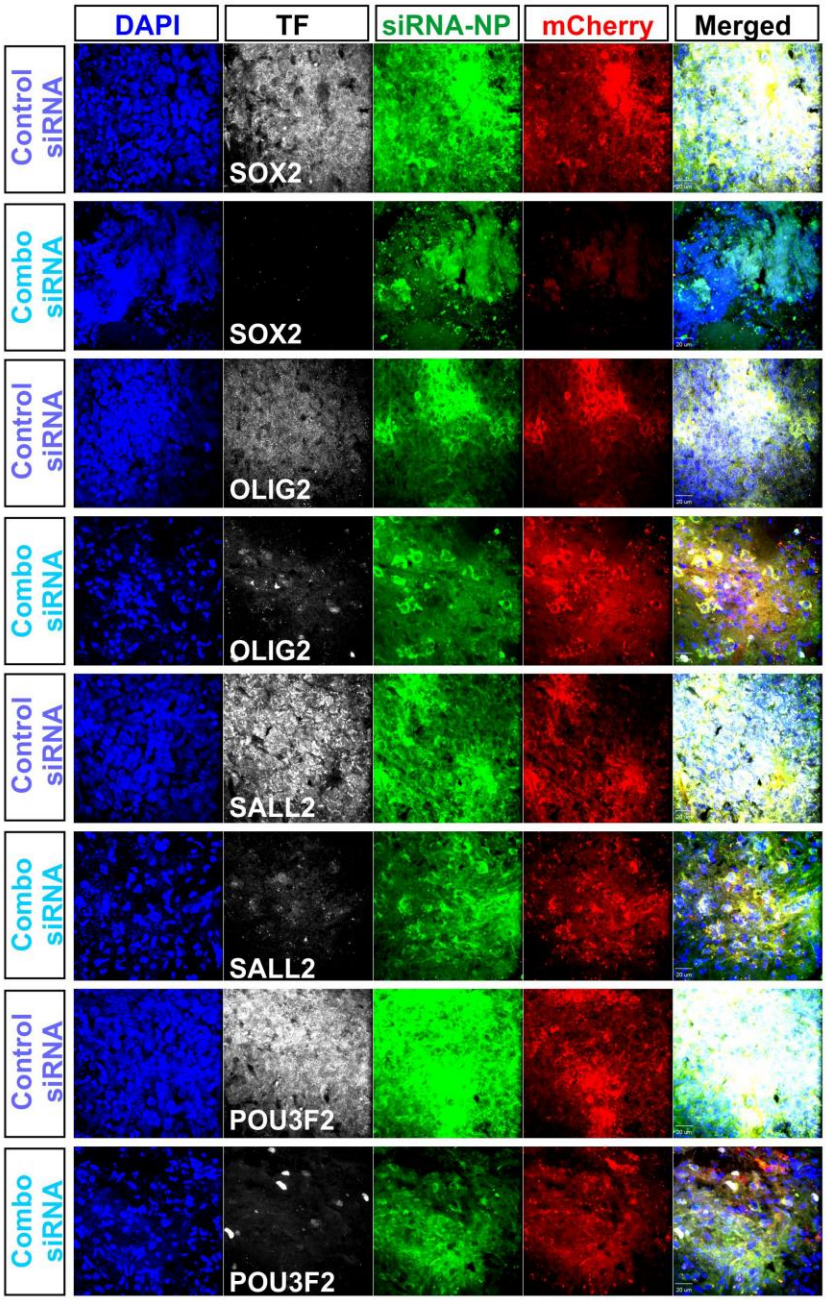

**Figure S10.** Laser Capture Microdissection (LCM) and quantitative reverse transcription polymerase chain reaction (qRT-PCR) analysis of *in vivo* impact of combo siRNA-LPNP complex infusion. **A**. Representative images of the injection site for tumor-bearing mouse brains, and LCM tissue cutting. The needle passage left behind a hole (yellow asterisk) in the axial section of the brain tissue. FAM (fluorescein)-tagged siRNA renders the LPNPs green, thereby demonstrates the diffusion distance from the injection site. **B**. Representative images of the infusion site for tumor-bearing mouse brains, and LCM tissue cutting strategy. Multiple cutting elements were used to pool the FAM+ tumor tissue. **C**. The representative tumor tissue selected for analysis was verified post-LCM with hematoxylin & eosin stain, where the cut tissue left behind a void (*). Green box is the site of image sampling for images in **B**. **D**. Comparison between LPNP-control siRNA and LPNP-combo siRNA treatments indicate significant reduction in TF mRNA levels after LPNP-combo siRNA infusion. **E**. There is significant differences in the tumor tissue distribution area between 3x injections and osmotic pump infusion (***$p$<0.001, $t$ test).

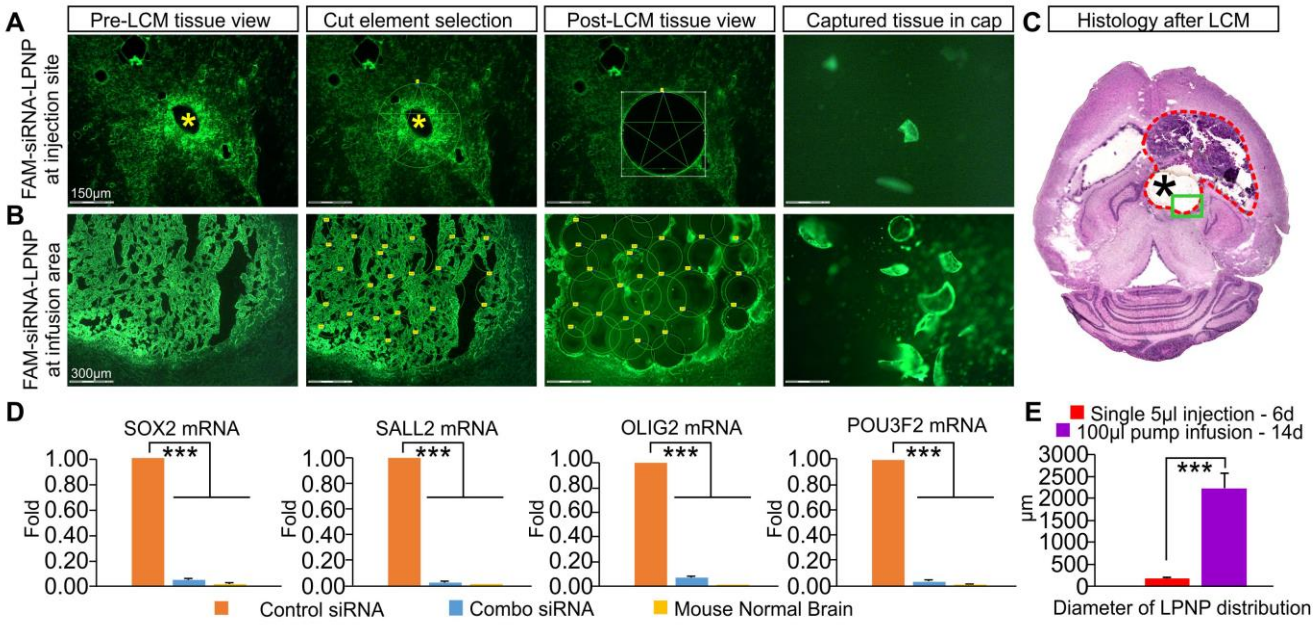

**Figure S11** Single cell sorting and Extreme Limiting Dilution Assay (ELDA) 96 well plate set up. **A**. Screen shot of the sorting scheme in the FACS Chorus™ software. **B**. Representative well images of sorted cells in ascending numbers (1, 3, 6, 12, 25, 50, 100, 200). Boxed areas are visually verified number of cells under microscope. **C.** Representative images of control siRNA treated MGG8 BTICs, with characteristic sphere formation with 7 days of treatment (left panel), and MGG8 BTICs treated with siRNA or LPNP-siRNA complexes (right panel), where adherent growth patterns and unhealthy appearances of cells were generally observed after 2 weeks of treatment with TF combo siRNAs. **D**. Representative dilution series of BTICs, and the ELDA results. Blue boxes indicate no tumor sphere observed, registered as a negative response, whereas, red boxes indicate sphere formation, hence, a positive response. Red arrows indicate tumor sphere formation.